Physical Properties of Nanostructure Sno_2 Thin Films Growth on Al_2O_3 Substrate by Pulsed Laser Deposition

Dr. Kasem Salman Kasem
Applied Sciences, University Of Technology/ Baghdad
Email:KAssim-Since@yahoo.com

Received on: 28/11/2013 & Accepted on: 6/2/2014

ABSTRACT

In this paper, the synthesis of nanostructure tin oxide SnO_2 thin films on (0001) sapphire substrates using a pulsed 532 nm Nd: YAG laser is presented. Deposition of films is achieved at three different substrate temperatures 300,400,500°C. The influence of substrate temperature on the structural and optical properties of tin oxide films are discussed and analyzed. We have shown the results of x-ray diffraction that all films prepared with the installation of multi crystalline (tetragonal) and directional prevalent (101) for all modds before and after annealing. These films are highly transparent (63–79%) in visible region, and transmittance of the films depends on substrate temperature. The band gap of the films varies from 3.45 eV to 3.61 eV for various temperatures. The morphology of deposited films was characterized by scanning electron microscope (SEM) and atomic force microscope (AFM), with increasing substrate temperature, both the grain size and surface roughness increase.

We have also investigated the photoluminescence (PL) emission of the simples produced by PLD. The absorption of very intense PL emission for the films at temperature T= 500 °C. The photoluminescence (PL) spectrum of the SnO_2 exhibits visible light emission with a peak at 602 nm.

Keywords: Pulsed Laser Deposition (PLD), Sno_2 Thin Films Nanostructures**.**

الخصائص الفيزياوية لاغشيةاوكسيد القصدير النانوية المنماة على قاعدة من الالومينا بطريقة الترسيب بالليزر النبضي

الخلاصة

في هذا البحث تم استعمال ليزر نيديميوم ياك النبضي ذو الطول الموجي(532 nm) ويعمل بتقنية عامل النوعية لترسيب اغشية اوكسيد القصدير النانوية على قواعد من الالومينا (0001) وبدرجات حرارية مختلفة (300,400,500)°C . تم مناقشة وتحليل تاثير درجة حرارة القاعدة على الخصائص التركيبية والبصرية لاغشية اوكسيد القصدير . اظهرت نتائج حيود الاشعة السينية ان جميع الاغشية المحضرة ذات تركيب رباعي متعدد التبلور وذات اتجاهية (101) لكافة النماذج قبل وبعد التلدين. امتلك الغشاء نفاذية عالية بالمنطقة المرئية بحدود 63-79 % واعتمدت النفاذية على درجة الحرارة القاعدة . تراوحت قيمة فجوة الطاقة من 3.45 eV- 3.61لمختلف درجات الحرارة. تم دراسة طبوغرافية السطح باستخدام المجهر الالكتروني الماسح (SEM) ومجهر القوى الذرية (AFM)ادت زيادة درجة حرارة القاعدة الى زيادة كلا" من خشونة السطح والحجم الحبيبي للجسيمات النانوية. اظهرت نتائج شدة الاضاءة الفوتونية للاغشية المصنعة بطريقة الترسيب بالليزر

النبضي شدة انبعاثية عالية عند درجة حرارة قاعدة 500 مئوي , الانبعاثية الضوئيةلاغشية اوكسيد القصدير كانت عند الطول الموجي 602 نانو متر.

INTRODUCTION

SnO_2 is a semiconducting of interest for technologically applications such as gas sensors, transparent electrical contacts or optoelectronics. Its electrical conduction is related to nonstoichiometry due to a large concentration of oxygen vacancies acting as shallow donors close to the conduction band.[1,2] However, this vacancy model seems to raise few fundamental questions to the general understanding of the phenomenon of transparent conductivity. Some theoretical results point out to an important role of the Sn interstitial which presents unusual stability due to the multivalence of tin under different chemical potential conditions in SnO_2. The latter class of oxides, namely semiconductors, has emerged as particularly interesting for sensors, thin-film electronics, and photonics. Tin oxide (SnO_2) is a wide band gap (3.6 eV) metal oxide semiconductor with excellent optical transparency in the visible range [3, 4, 5, 6, 7, and 8]. It possesses the rutile (tetragonal) crystal structure with a = 4.738A˚ and c = 3.188A˚ .With a relatively high conductivity, visible wavelength transparency, chemical stability and thermal stability in oxidizing environments [9], tin oxide films are being explored for a number of applications. As a wide bandgap semiconductor, SnO_2 is attractive for use in photonic applications, such as solar cells, where transparent electrodes are required [10, 11].

SnO_2 thin films are used for gas sensor devices based on changes in conductivity when exposed to selected chemical species [12–17]. In addition, there is also interest in the possibility of inducing ferromagnetism in SnO_2 through transition metal doping [18, 19], an approach that is also being pursued for other wide bandgap semiconductors [20– 22]. SnO_2 thin films have been fabricated by a variety of techniques including sol–gel method [23], electron beam evaporation [24], reactive sputtering [25] chemical vapor deposition and sputtering [26]. One of the major challenges in synthesizing SnO_2 thin films is to control oxygen stoichiometry. When deposition is carried out in vacuum at high temperatures, SnO_2 films tend to be nonstoichiometric, frequently resulting in the formation of metastable phases such as SnO or Sn_3O_4 [27,28,29]. The existence of these metastable phases and relaxed crystal defects will strongly affect the properties of the films. While previous applications of SnO_2 for sensors or transparent conductors have primarily relied on polycrystalline material, many of the emerging applications for functional wide band gap semiconductors require highly crystalline films. Pulsed laser deposition has the advantage of operating in a reactive atmosphere over a wide range of oxygen pressure. In this paper, the synthesis of nanocrystalline tin oxide SnO_2 thin films on on (0 0 0 1) sapphire substrates using a pulsed 532 nm Nd: YAG laser is presented.

Deposition of films is achieved at three different substrate temperatures 300,400,500°C. The photoluminescence (PL) spectrum of the SnO_2 exhibits visible light emission with a peak at 602 nm.

EXPERIMENTAL PROCEDURE

Film preparation

The deposition was carried out using a Q- switched Nd:YAG laser with a frequency second harmonic generation at 532nm (pulse width 7nsec repetition rate

10HZ) and fluencies energy 1.5 J/cm ^{2} . The studied films were prepared by from pure SnO_2 targets films were grown by pulsed laser deposition on sapphire (Al_2O_3) (0 0 0 1) substrates kept an on-axis distance of 4cm from the SnO_2 target. The chamber was kept at vacuum pressure of 10^{-5} mbar as shown in Figure (1). The SnO_2 disc was ablated from 10-100 pulses (10-20min) to get single layered thin films with thickness 200 nm. During the deposition the substrate temperatures (Ts) were variable from (300-500 $^\circ$C).

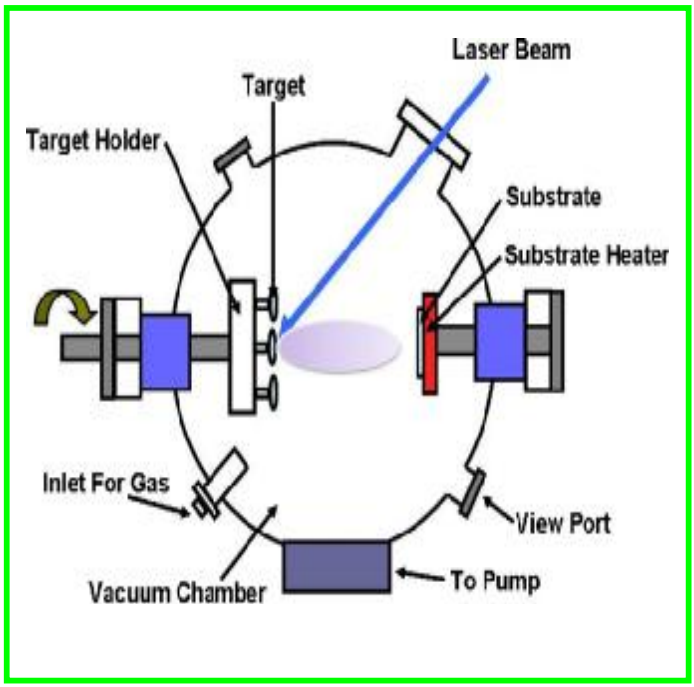

Figure (1) Schematic diagram of pulsed laser deposition system.

Film characterization

The crystalline structure of the films was determined by X-Ray Diffraction (XRD) measurements (Philips PW 1050, λ=1.54A$^\circ$) using Cu kα . Optical transmission and absorption spectra of all the films were recorded using a UV-VIS (Perkin Elemer Company) spectrophotometer, in the spectral range of (300-900) nm. The surface morphology was examined by scanning electron microscopy (SEM–JEOL 7000) and by atomic force microscopy (AFM-Digital Instruments NanoScope) working in tapping mode. The photoluminescence is the optical emission obtained used He-Cd laser (325 nm) as the excitation source. Using the luminescence LS55 devise in Malaysia.

RESULT AND DISCUSSION

SnO_2 films prepared under 10^{-1} torr oxygen pressure, (300-500)$^\circ$C substrate temperature and 1.2 J/cm^2 laser fluence on Sapphire (Al_2O_3) substrate are shown in Figure (2) .Shows the XRD patterns of the films at substrate temperature 300, 400

and 500°C, respectively. All the films consisted of SnO_2 of tetragonal structure. With increasing the substrate temperature, peak intensities in each thin film increased gradually. Especially as substrate temperature 300°C although the position of a broad peak (211) indicating was shifted to higher angle those mean that the crystallinities of the films were improved with increase of substrate temperature. Here, it is worth noting that no microstructural change occurred significantly in the films substrate temperature at 500 °C. In the substrate temperature less than 500 °C, increasing the substrate temperature gives rise to the improvement of crystallinity in the films substrate temperature at 500 °C without a big microstructure change. The weak peaks for SnO_2 (101) grains are also observed at higher substrate temperature. The results clearly show that deposited SnO_2 grains on the (0001) Al_2O_3 substrate is favored, placing the film c-axis in the plane of the surface.

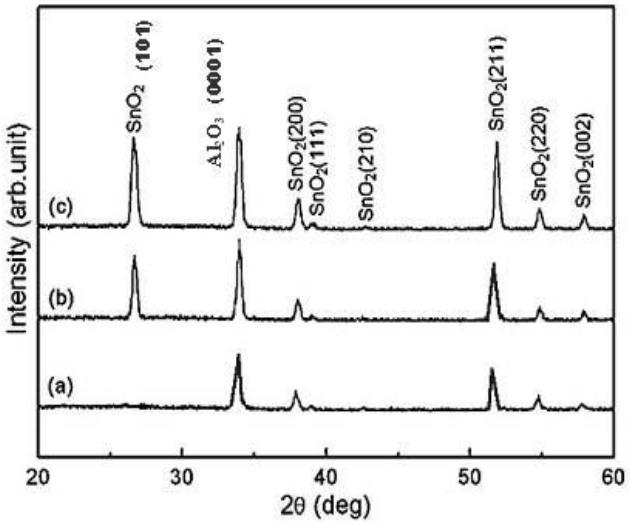

Figure (2) XRD patterns of SnO_2 film grown at different Temperatures on Al_2O_3

Figure (3) shows the AFM images of the SnO_2 thin films deposited at substrate temperatures of (300, 400 and 500) °C. The surface morphology of the SnO_2 thin films as observed from the AFM micrographs proves that the grains are uniformly distributed within the scanning area (10 x 10 μm^2), with individual columnar grains extending upwards. This surface characteristic is important for applications such as gas sensors and catalysts [19, 23].

From the topographic images it can be seen that the films deposited at 300 °C appears to be more uniform than the topography of the sample deposited at 400 and 500°C. The RMS roughness also increased with increasing substrate temperatures (Ts), the section analysis shows that RMS roughness values are (98.84 ,138.35 and 120.44 nm) for thin films deposited at (300 , 400 and 500)°C respectively. A possible explanation for this observation is that surface mobility of the adatoms is higher at temperature (500 °C), these results in higher surface diffusion length, island separation, and lateral size. When island separation length is greater than the lateral size of the island, terrace and stairs topography are normally favored. On the other

hand, surface mobility of the ad atoms are lower at lower temperature (300 ˚C), thus islands are more closely spaced. If island separation is smaller than the island lateral size, more uniform growth of the thin film is preferred.

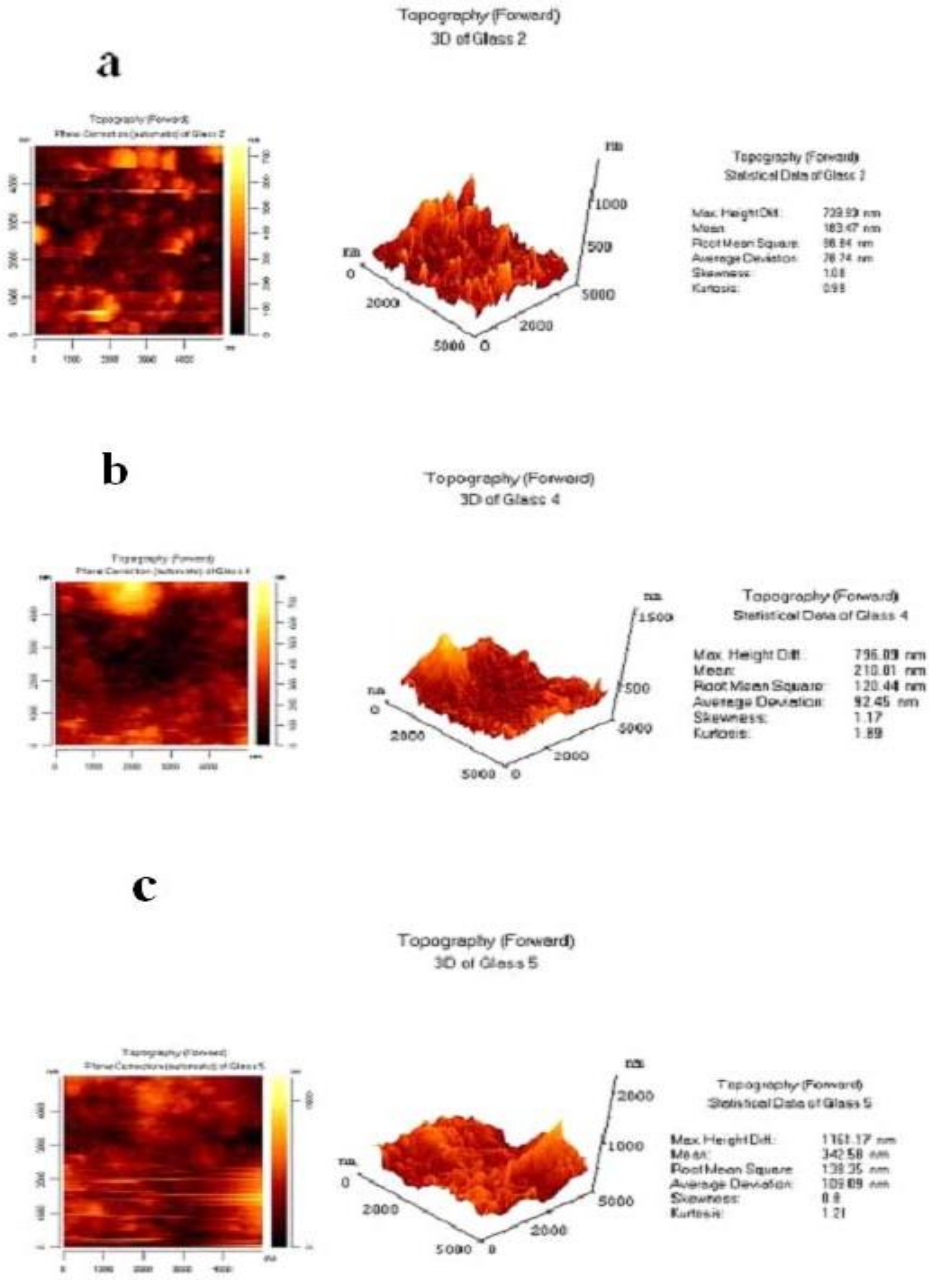

Figure (3) AFM image of SnO_2 film grown at different temperatures on Al_2O_3 a) 300 ˚C ,b) 400 ˚C , c) 500 ˚C

SEM micrographs in Figure (4) showing the effect of substrate temperature on the microstructure of thin films. All the microstructures revealed that the thin films are very porous and not uniform locally. The film has homogeneous surface morphology and with increasing substrate temperature Ts, the grain size of aggregated particles increases ,grain size values are (46 ,68.5 and 130. 4 nm) for thin films deposited at (300 , 400 and 500)°C respectively.

In those films, the apparent particle size on the microstructures seems to be about 45–50 nm, of which the particle size is slightly coarser than that of as-oxidized powder, but is different to the particle size of 58–68 nm calculated from the specific surface area. The difference may be attributed to a fact that the particle size maximum value because the area aggregated between particles is not considered.

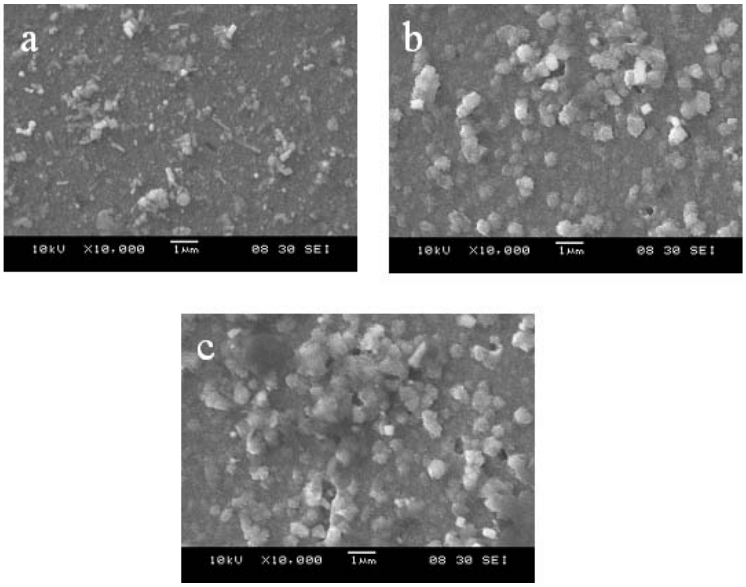

Figure (4) SEM images of SnO_2 films at at different temperatures on Al_2O_3 a) 300 °C ,b) 400 °C , c) 500 °C and had thickness200 nm.

Figure (5) shows the effect of substrate temperature on optical transmittance of SnO_2 thin films. It has been observed that optical transparency of the films increases with increases in temperature. The average percentage transmittance in the range of 450–900 nm is 63%, 70% and 79% for the films grown at 300°C, 400°C and 500°C respectively. The average transmittance is calculated by taking the average value of the transmittance over 450–900 nm range for each sample [11]. The effect of substrate temperature on optical band gap of SnO_2 thin films has been determined from the data of transmittance vs. wavelength plot. The absorption coefficient (α) is given by

$\alpha = \ln (1/T)/ d$ [1].

Where T is transmittance and d is film thickness 200 nm. The relation between the absorption coefficient and the incident photon energy (hα) is given by the following equation [12]:

$(\alpha h\nu)^2 = A(h\nu - Eg)$

Where A and Eg are constant and optical band gap, respectively. The Eg can be determined by extrapolations of the linear regions of the plots to zero absorption.

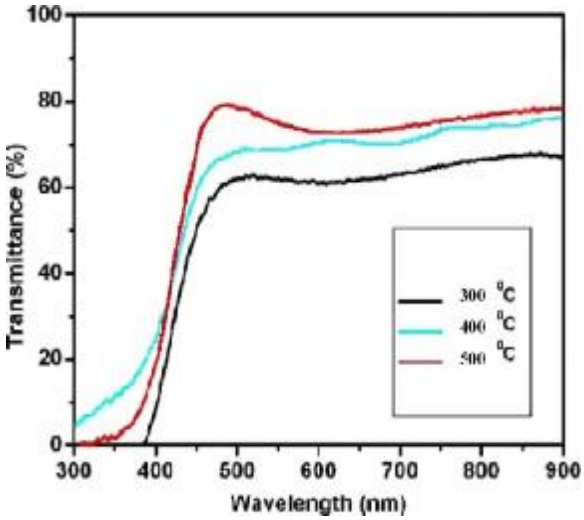

Figure (5) Transmittance spectra of SnO_2 films grown at different Substrate temperatures.

Figure (6) shows the relationship between $(\alpha h\nu)^2$ and hν for films grown at different substrate temperature. Substrate temperature having different effect leads to increase in the optical energy gap values, because the increasing substrate temperature process decreases from the secondary levels and the structure defects which lead to the contract tails region. This leads to expand in the optical energy gap It is observed that the band gap varies from 3.42 eV,3.49 eV and 3.61 eV for the films grown at 300°C, 400°C and 500°C respectively .

Figure (7) shows the room-temperature and 500°C substrate temperature photoluminescence spectrum of the as-prepared SnO_2 thin films. The photoluminescence (PL) spectrum of the SnO_2 exhibits visible light emission with a peak at 602 nm. The low-energy emission might be related to crystal defects or defect levels associated with oxygen vacancies, or tin interstitials that have formed during growth. A similar red emission has been reported in the case of SnO_2 thin films synthesized by laser ablation [14].At 500 °C substrate temperature the strong PL peak might be related to the crystalline defects induced during the growth. The oxygen vacancies interact with interfacial tin vacancies, and lead to the formation of a considerable amount of trapped states within the band gap, which results in a strong

PL signal. Similar results were also observed for SnO_2.[13] The optical measurements further show that the SnO_2 thin films possess surface characteristics that generate a red emission band that may be exploited in gas sensors or other optoelectronic devices [6].

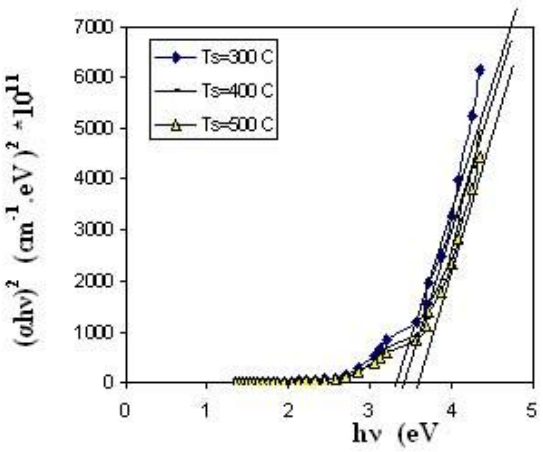

Figure (6) Plot of $(\alpha h\nu)^2$ against hν of of SnO_2 films grown at different temperatures.

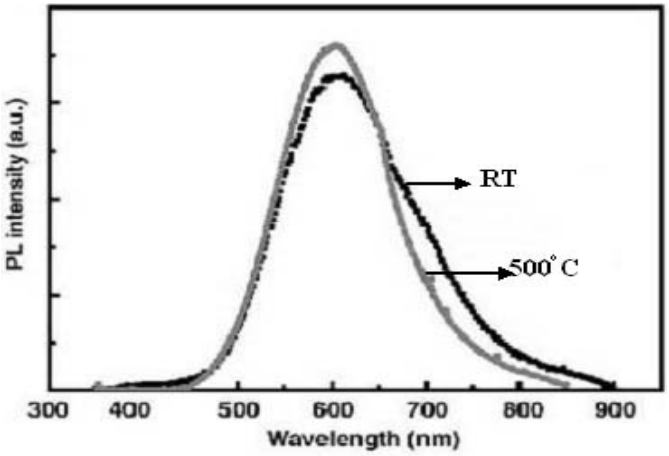

Figure (7) The photoluminescence spectra of SnO_2 thin films at two substrate temperatures.

REFERENCES

[1]. Heo, Y.W. Y.W. Kwon, Y. Li, S.J. Pearton, D.P. Norton, Appl. Phys. Lett. 84 (2004) 3474.

[2]. Pearton, S.J. D.P. Norton, K. Ip, Y.W. Heo, T. Steiner, Superlattices Microstruct. 34 (2003) 3.

[3]. Norton, K. Ip, Y.W. Heo, D.P. S.J. Pearton, J.R. LaRoche, F. Ren, Appl. Phys. Lett. 85 (2004) 1169.
[4]. Jeong, B.S. J.D. Budai, D.P. Norton, Thin Solid Films 422 (2002) 166.
[5]. Song, S.K. Phys. Rev. B 60 (1999) 11137.
[6]. Kim,W.J. W.H. Koo, S.J. Jo, C.S. Kim, H.K. Baik, J. Lee, S. Im, Appl. Surf. Sci. 252 (2005) 1332.
[7]. Rakhshani, A.E. Y. Makdisi, H.A. Ramazaniyan, J. Appl. Phys. 83 (1998) 1049.
[8]. Okuya, M. S. Kaneko, K. Hiroshima, I. Yagi, K. Murakami, J. Eur. Ceram. Soc. 21 (2001) 2099.
[9]. Lee,D.S. G.H. Rue, J.S. Huh, S.D. Choi, D.D. Lee, Sens. Actuators B 77 (2001) 90.
[10]. Rue, G.-H. D.H. Yoo, Y.H. Hwang, H.-K. Kim, J. Mater. Res. 17 (2002).
[11]. A. Khanna, R. Kumar, S.S. Bhatti, Appl. Phys. Lett. 82 (2003) 4388.
[12]. Kilic, C. A. Zunger, Phys. Rev. Lett. 88 (2002) 095501–95511.
Stampe, R.J. Kennedy, E.C. Moreira, U.S. Sias, Phys. Rev. B 74 (2006) 115307.
[13]. Punnoose,A. J. Hays, J. Appl. Phys. 97 (Part 2) (2005) 10D321.
[14]. The odoropoulou, N.A. A.F. Hebard, D.P. Norton, J.D. Budai, L.A. Boatner, J.S. Lee, Z.G. Khim, Y.D. Park, M.E. Overberg, S.J. Pearton, R.G. Wilson, Solid-State Electron. 47 (2003) 2231.
[15]. Ivill, M. S.J. Pearton, D.P. Norton, J. Kelly, A.F. Hebard, J. Appl. Phys. 97 (2005) 053904.
[16]. Pearton, S.J. C.R. Abernathy, G.T. Thaler, R.M. Frazier, D.P. Norton, F. Ren, Y.D. Park, J.M. Zavada, A. Buyanova, W.M. Chen, A.F. Hebard, J. Phys.-Condens. Matter 16 (2004) R209.
[17]. Frazier, K. Ip, R.M. Y.W. Heo, D.P. Norton, C.R. Abernathy, S.J. Pearton, J. Kelly, R.Rairigh, A.F. Hebard, J.M. Zavada, R.G. Wilson, J. Vac. Sci. Technol. B 21 (2003)1476.
[18]. Park, S.S. J.D. Mackenzie, Thin Solid Films 258 (1995) 268.
[19]. Choudhary, R.J. S.B. Ogale, S.R. Shinde, V.N. Kulkarni, T. Venkatesan, K.S. Harshavardhan, M.S.B. Hannoyer, Appl. Phys. Lett. 84 (2004) 1483.
[20]. Cavicchi, R.E. S. Semancik, M.D. Antonik, R.J. Lad, Appl. Phys. Lett. 61 (1992) 1921.
[21]. Kojima, M. H. Kato, A. Imai, A. Yoshida, J. Appl. Phys. 64 (1988) 1902.
[22]. Liu, D. Q. Wang, H.L.M. Chang, H. Chen, J. Mater. Res. 10 (1995).
[23]. Park,Y.R. K.J. Kim, J. Appl. Phys. 94 (2003) 6401.
[24]. Goodchild, R.G. J.B. Webb, D.F. Williams, J. Appl. Phys. 57 (1985) 2308.
[25]. Pan,X.Q. L. Fu, J. Appl. Phys. 89 (2001) 6048.
[26]. Lowndes,D.H. D.K. Christen, C.E. Klabunde, Z.L. Wang, D.M. Kroeger, J.D. Budai, S. Zhu, D.P. Norton, Phys. Rev. Lett. 74 (1995) 2355.
[27]. Budai, J.D. W.G. Yang, N. Tamura, J.S. Chung, J.Z. Tischler, B.C. Larson, G.E. Ice, C. Park, D.P. Norton, Nat. Mater. 2 (2003) 487.
[28]. Usui H, Sasaki T, Koshizaki N. Effect of Alkyl Chain Length on Layered Structure of Sn Nanocomposites [J]. Chemlett, 2012, 34: 700.
[29]. Kandori K, Kon-No K, Kitahara A. Formation of Ionic Water Oil Micro emulsions and Their Application In The Preparation of Tio_2 Particles [J]. J Colloid Interface Sci, 2013, 122: 78−82.